Available online at www.sciencedirect.com
SCIENCE DIRECT®
Journal of Loss Prevention in the Process Industries 16 (2003) 209–221
Journal of Loss Prevention in the process industries
www.elsevier.com/locate/jlp

# Investigation of the Fushun ASU explosion in 1997

J.-Y. Lehman [a,*], X.C. Wei [b], Q.X. Hua [b], G. Delannoy [c]

[a] *Air Liquide, France*
[b] *Fushun Petrochemical Company, No. 2 Refinery, China*
[c] *SME (SNPE Matériaux Energétiques), France*

**Abstract**

On the 16 May 1997 an explosion occurred at the Fushun Ethylene Complex, in Fushun, Liaoning province, China. The explosion source was located in the distillation column of the air separation nunit of the complex. The explosion was extremely severe causing the death of four people, injuring four severely and 27 slightly, and causing extensive material damage.

A number of possible pollution sources was investigated. The remains of the low pressure column and of the main vaporiser were reassembled. A model was developed to understand ignition of aluminium when polluted by combustible material in liquid oxygen. Laboratory tests were made on ignition of polluted aluminium in LOX. Ethylene dispersion in the atmosphere was also modelled.

It can be concluded that the accident resulted from an exceptional pollution peak due to venting of ethylene during a shut down of the ethylene oxide plant, together with a temporarily low liquid level in the main vaporiser of the air separation unit at reduced load.

The hydrocarbon pollutant acted as an igniter, the actual fuel was aluminium. Calculations show that a few hundreds grams of ethylene were able to ignite more than 1000 kg of aluminium in liquid oxygnen, multiplying the explosion energy by more than 1000.


*Keywords*: Explosion; Aluminium; Oxygen; Contamination; Air separation



## 1. Introduction

On the 16 May 1997 at 9.05 a.m. a powerful explosion occurred at the Fushun Ethylene Complex, in Fushun, Liaoning province, China. The explosion source was located in the distillation column of the air separation unit (ASU) of the complex (Fig. 1). The explosion was extremely severe causing the death of four people, injuring four severely and 27 slightly, and causing extensive material damage.

After the explosion an investigation was undertaken by the operating company (Fushun Ethylene Chemical Co, FEC) with the help of the air separation plant supplier (Air Liquide, AL) and of a French explosion expert company (Société Nationale des Poudres et Explosifs,

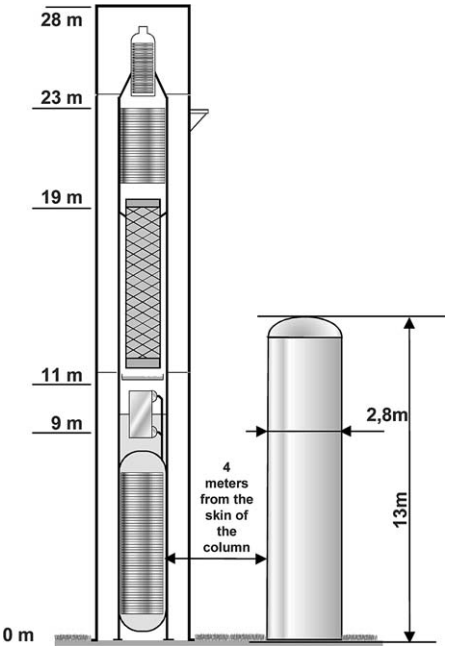


Fig. 1. Sketch of distillation column and liquid nitrogen tank.

* Corresponding author. Consultant. Retired from Air Liquide, France. Tel. and fax: +1-33-143-68-64-38. Postal address: 27, Domaine de Chateau Gaillard, Maisons Alfort, 94700, France.

0950-4230/03/$ - see front matter © 2003 Elsevier Science Ltd. All rights reserved.
doi:10.1016/S0950-4230(02)00110-9

SNPE). This paper describes the investigation and the results.[1]

## 2. Plant characteristics

The plant capacity was 200 t/d oxygen at 99.8% purity with 6000 $Nm^3/h$ gaseous oxygen (GOX), 6000 $Nm^3/h$ gaseous nitrogen (GAN) (both produced at low pressure and compressed in product compressors), 100 $Nm^3/h$ liquid oxygen (LOX) or liquid nitrogen (LIN). The ASU had been designed in 1988 and commissioned in 1991 and had been running satisfactorily since that date. It was located in the Fushun Ethylene Chemical complex, east of the ethylene oxide and ethylene glycol plants. It incorporated the following particular features: front end purification (double beds: alumina and molecular sieve), LOX adsorber (silicagel), bath type main reboiler condenser (two brazed aluminium heat exchangers (BAHX) cores with common nitrogen headers), two expanders. The lower section of the low pressure column consisted of aluminium structured packings fitted in an internal shell. LOX was circulated through the LOX silicagel adsorber by means of an additional vaporiser heated by rich liquid.

## 3. Accident and damages

Four persons were killed, four severely injured and 27 slightly injured.

In the cold box only the high pressure column as well as a part of the main exchangers were still standing. The walls of the compressor buildings located next to the cold box were blown up and a pipe rack located nearby was bent by a vertical liquid nitrogen storage tank falling down (Fig. 2). The cold box casing had disintegrated.

One person was knocked on the head and killed by a casing plate, which fell 200 m away from the ASU. Extensive damage was caused to equipment and buildings located around the column and all glass windows of the buildings within a radius of 200 m were broken, and 50% within a radius of 300 m. A 370 kg beam belonging to the cold box structure was found about 600 m away from the ASU. According to our knowledge, this accident was by far the most severe explosion that had ever occurred in an ASU at that time.

## 4. Circumstances of the accident

Six hours before the explosion, the ethylene oxide plant was shut down and gas was vented during these 6 h. The gas composition was 31% ethylene, 48% methane, 6% $CO_2$, the rest being oxygen and nitrogen. Its flow rate was 700 to 500 $Nm^3/h$. The venting point was located at the top of a column of the ethylene oxide plant, 103 m west of the ASU air compressor intake and 40 m high above ground. The ASU air intake is 31 m high. The wind was blowing in an unusual direction, from the venting point toward the ASU air intake.

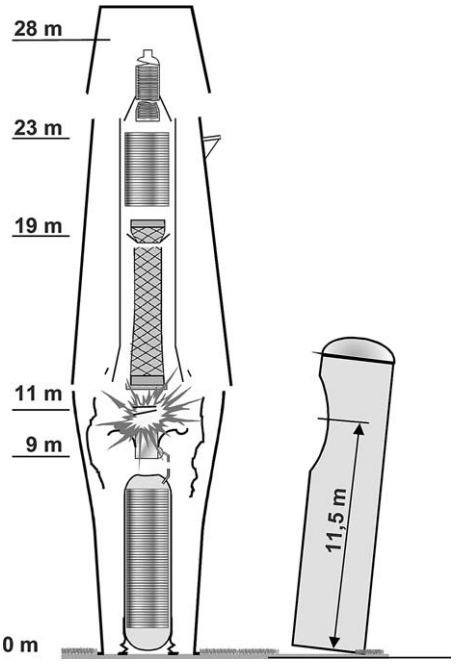


Fig. 2. First phase (explosion): effect on the adjacent nitrogen storage tank.

Due to the shutdown of the ethylene oxide plant, the ASU was producing nitrogen and oxygen, gaseous oxygen being vented and the air compressor was running at 80% load. Nine hours before the explosion the main condenser liquid level was decreased to down to 50 to 60% core submergence. The plant had produced no LOX for some time. The hydrocarbon content in the sump before the venting started was unknown as hydrocarbons were not analysed. Other sources of impurities in the atmospheric air, in the cooling water, or in other fluid circuits cannot be excluded.

## 5. Detailed investigation

The purpose of the investigation was to understand the causes and to quantify the effects of the explosion.

A series of various independent investigations were conducted in parallel by different teams:

- Reassembly of the low pressure column;
- Reassembly of the vaporiser;
- Collection of data in order to assess the explosion power.

[1] One incident with comparable consequences has been reported in van Hardeveld et al., 2001.

Operating records were examined and a number of possible pollution sources were also investigated such as cross pollution of utility networks. The possibilities of sending hydrocarbons to the air/water column upstream of the purification unit, of sending back up instrument air to the process air were successively studied and eliminated.

Adsorbents were analysed: traces of ethylene were found in the molecular sieve from the front end purification and in the silicagel from the LOX adsorber. The finding of only traces of ethylene can be explained by the fact that the silicagel samples were taken after a long exposure to ambient air through broken piping after the explosion.

Then studies were launched in parallel in order to understand the various aspects and to come to a conclusion:

- Explosion power assessment;
- Modelling of aluminium ignition in LOX;
- Laboratory tests on promoted ignition of aluminium in LOX;
- Assessment of the quantity of pollutant required to lead to a massive aluminium ignition;
- Simulation of ethylene dispersion;
- Process calculations to map the pollutant concentration in the vaporiser.

These various approaches are discussed below.



## 6. Reassembly of the column, possible explosion scenario

All parts belonging to the column, pressure vessel, internals and main reboiler, were collected, identified as far as possible and reassembled on the ground in order to compare the remains to the original state. The corresponding observations made are shown on Figs. 3 and 4.

### *6.1. Low pressure (LP) column*

The following fractions were recovered:

- Main condenser shell: 12 $m^2$ out of 18.3 $m^2$, 66%;
- Oxygen section inner and outer shells: about 11 $m^2$ out of 83 $m^2$, 13%, packing: 1%;
- Waste nitrogen section shell: 16.8 $m^2$ out of 28 $m^2$, 61%;
- Pure nitrogen section shell: 100%;
- Trays: 100 %.

Other observations:

- Main condenser shell: crumpled aspect, black traces inside, no burn, showing: cold deformation);

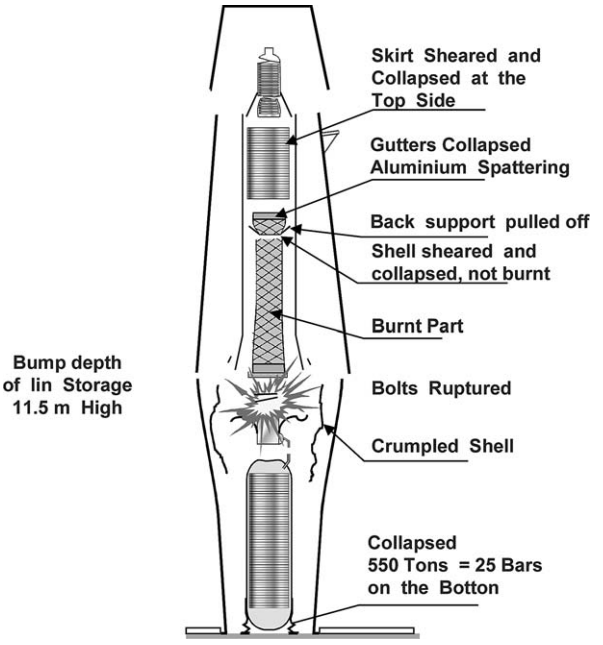


Fig. 3. First phase (explosion).

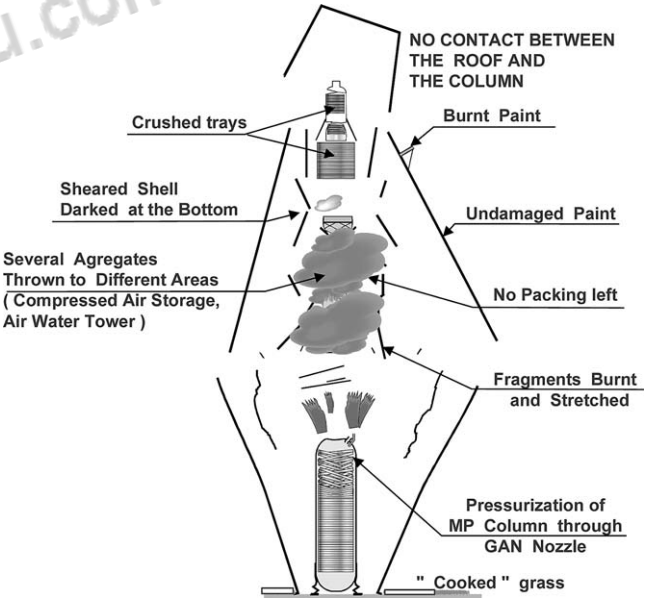


Fig. 4. Second phase (packings combustion).

- Oxygen section outer shell: small pieces, burnt;
- Waste nitrogen section shell: inner skirt cut off from its conical head, buckled inwards at upper end;
- Liquid distributor and connected parts: troughs collapsed inwards;
- Inner shell cut at the junction cone level and the remaining part buckled inwards, aluminium projections on lower side, local burns, upper side unburned.
- Lower part of the inner stainless steel shell almost totally burnt.

### 6.2. Zoom on the rich liquid distributor

The lower part of the LP column (i.e. below the rich liquid feed) was filled with packing, which was fitted in an inner shell connected to the outer shell by means of a cone. It could be observed that the inner shell had been cut at the welding joint with this cone by the blast wave before the combustion reached this point, the inner shell was burnt below this cut, but not above. This seems to indicate that there were two events: an explosion in the reboiler, which dislocated the column, and then a fire, which burned the packings.

### 6.3. Interpretation

The most probable scenario of the column explosion would be the following (Figs. 2 to 4): the first event was the violent explosion of the main condenser, which dislocated the LP column into several sections as well as the casing, the pure nitrogen section was blown away, the upper part of the LP column shell was ruptured, and then the lower section of the LP column (shell and internals) burnt with a large heat release and limited pressure blast.

## 7. Reassembly of the reboiler

As it was the part in which the explosion was initiated, the reboiler was reassembled separately. It had exploded into six 'slices'(Fig. 5). 'Slice 2' was missing but the other five slices were satisfactorily identified. The five recovered 'slices' had a total weight of 1160 kg (the original weight was 2900 kg, 1700 kg aluminium had disappeared).

Generally speaking it could be observed that the edge opposite to the gaseous nitrogen header had disappeared ('slice 1') or had been 'opened' like the pages of a book


Fig. 6. Vaporiser remains, reassembly.

('slice 6', see Fig. 6). It strongly suggests that the explosion started from that particular zone. The combustion did not reach the bottom of the recovered cores except in one layer.

In the least burnt parts (e.g. in 'slice 6') it could be seen that the fins had disappeared in the oxygen layers leaving naked unburned parting sheets, showing independent propagation of combustion in a layer burning the thinner parts to start with, from the origin edge to the rest of the layer (Figs. 7 and 8).

### 7.1. Questions

This raised the following question: how can aluminium combustion start in different layers without the parting sheets being pierced, i.e. without direct firing?

An explanation is that the shock wave caused by the explosion of one layer can ignite next layers (Figs. 8 and 9). An obvious objection to this is that ignition of 0.2 mm aluminium foils in LOX by shock is very difficult as it requires a very high amount of energy. But what

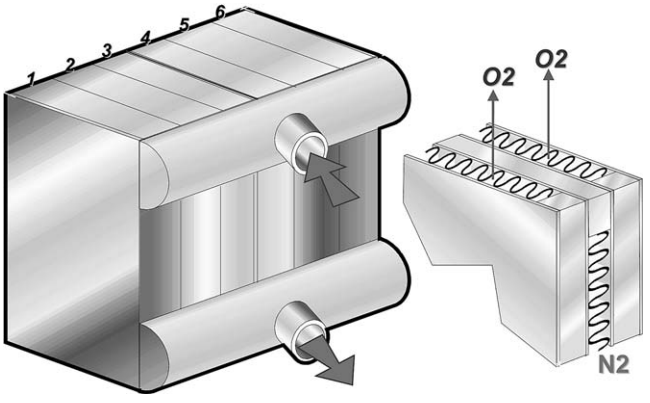


Fig. 5. Vaporiser rupture in six 'slices'.

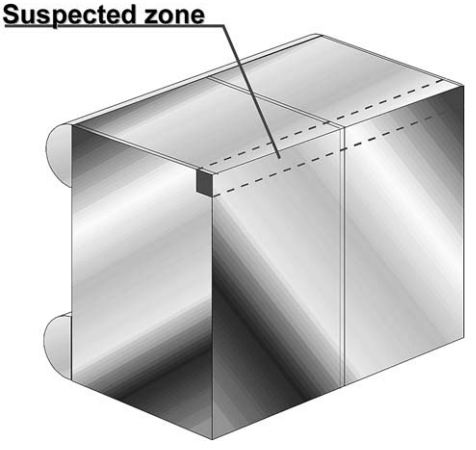


Fig. 7. Explosion starting zone.

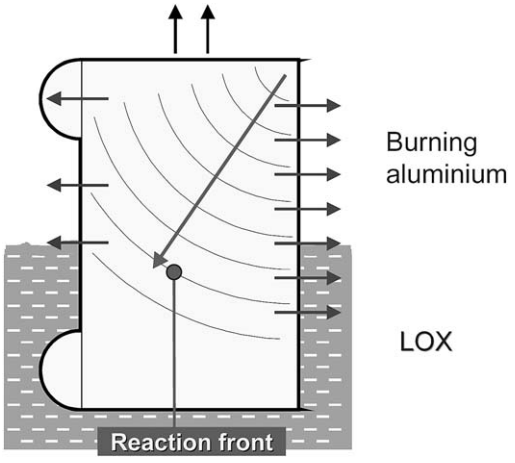


Fig. 8. Combustion propagation within a passage.

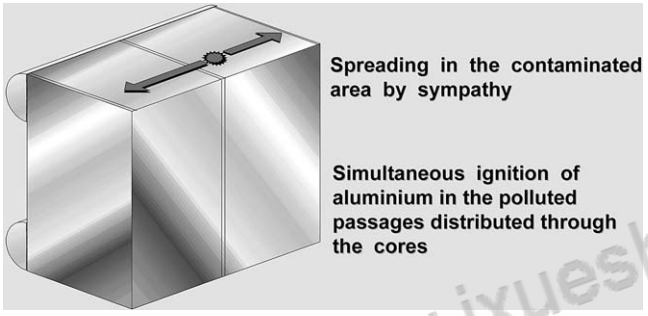


Fig. 9. Propagation from passage to passage.

happens if they are coated with hydrocarbons? This will be discussed later.

## 8. Additional data regarding the explosion

### *8.1. Structural damage outside the LP column*

The lower part of the column (high pressure column) was not destroyed. It was only 'weakly' damaged: the top of its upper head was bumped and its support skirt was buckled. A vertical liquid nitrogen tank located next to the cold box fell down and the upper part in front of the column was bumped at 11 m altitude. The molecular sieve adsorbers were not damaged. The tall water wash column (CT650) tower was pushed by the blast wave and six anchor bolts failed. It did not fall down but it remained only tilted (the two remaining bolts still holding it on its base).

No impact of possible primary fragments was observed either on the debris or on the neighbouring equipment. Practically no traces of burned paint were found on the cold box casing (exceptional places only, i.e. green part at the end of flying piece No. 47: mid-section of main vertical beam with platform support).

The debris map established by FEC shows that very few pieces were thrown in the sector delimited by the N-W and S-W directions, with larger effects important in the East direction. As shown on the map of main steel pieces, the 12 m high beam of the N-W post of the cold box has not been recovered and the 12 m high beam of the S-W post was recovered in the S-E direction.

### *8.2. Window glass breakage*

Many of the glass windows were broken both inside and outside the complex at great distance. FEC estimated the percentage of damaged glass windows for all buildings. See Fig. 10.

### *8.3. Ear-drum ruptures*

Two seriously injured people had one ear drum ruptured. This can give an indication regarding the maximum overpressure of the blast.

### *8.4. Witnesses*

When the explosion occurred, a worker was riding on a bicycle at about 60 m from the explosion centre in the north direction. He was hurled by the blast wave and was thrown away between 13 and 18 m. He was not injured and the investigation team met him in order to record its testimony. This eyewitness stated that he felt a 'big warm blast' on his back. He also stated that the explosion sound was rather a 'very long blast' than a 'short bang'.

A person was by chance taking pictures in a building 3 km away from the plant. When he heard the bang, he climbed to the top floor and took a picture about 1.5 min after the explosion showing a 300 m diameter white cloud about 300 m above ground.

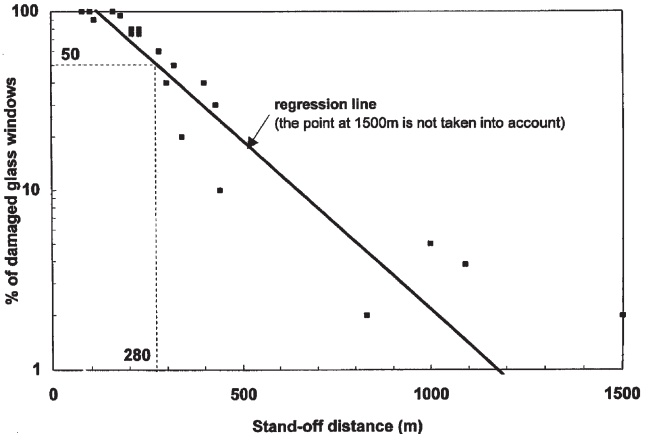


Fig. 10. Percentage of damaged glass window vs. stand-off distance.

## 9. Explosion power assessment

### 9.1. Introduction

It has been noted early that the chemical energy, E, is an important feature of an explosion source. It is the most important parameter in describing and assessing the severity of an explosion. Unfortunately, this quantity has often proved quite difficult to estimate for accidental non-ideal detonations (an ideal detonation has a zero reaction time), although it is well known for given masses or volumes of chemical high explosives.

It has been common practice in the evaluation of blast wave damage from accidental explosion to express the severity of the damage caused by the explosions in terms of its 'TNT equivalency', i.e. in terms of how many kilograms of TNT would do an equivalent amount of damage. What one is in fact doing is equating the blast wave strength to that from an equivalent mass of TNT. That this is not an exact procedure should be clear from the comparisons of blast waves from TNT and other explosion sources. It is reasonably correct for other chemical high explosives and in the far-field for sources with lower energy density. However, in order to give an assessment of the explosion power level, it is proposed to determine the weight of TNT which would be required to get the observed amount of damage at that distance from the centre of the explosion for some blast effects.

These blast effects are listed in Table 1.

### 9.2. Window glass breakage

In most buildings, the components which normally fail at the lower blast loads are windows. Window glass is a brittle material which will shatter when stress reaches the elastic limit. In order to predict the glass breakage load and the size and the velocity of glass fragments, some authors propose computation methods. Unfortunately these methods are complex and require many parameters such as:

- Pane dimensions and thickness;
- Type of glass;
- Type of frame;
- Position of the window with regard to the blast wave propagation;
- Location and size of glass fragments recovered after explosion, etc.

Table 1
Distance between blast effects and explosion centre

| Blast effect | Horizontal stand-off distance (m) |
|---|---|
| Window glass breakage | 80 to 1500 |
| Motion of the witness riding a bike | 60.0 |
| Ear-drum rupture (two injured people) | 35.0 |
| Tilting of the CT607 tower | 18.5 |
| Flying of steel piece No. 47 (main post of the cold box) | 7.6 |
| Structural damage to the lower part of the column | 0.0 |

A statistical method was used. The French Standard 11300 gives a such statistical method.(Fig. 11) On the incident overpressure vs. stand-off distance diagram there are two curves corresponding to 50% of damaged glass windows. As shown in annex 6, the regression line fitted on data gives a stand-off distance of 280 m for 50% of damaged glass windows (Fig. 10). For this stand-off distance the results are as follows (see Fig. 11): Curve 1 gives $Ps = 4\times10^3$ Pa and QTNT 1000 kg, curve 2 gives $6 \times 10^3$ Pa and QTNT = 2000 kg. (Ps, incident overpressure; QTNT, mass of the free-field spherical TNT charge required to get Ps at 280 m.)

### 9.3. Ear-drum rupture

The state-of-art for predicting ear-drum rupture is not as well developed as that for predicting lung damage from blast waves. A direct relationship, however, has been established between the percentage of ruptured ear-drums and maximum overpressure (Hirsh, 1968). According this relationship, 50% of exposed ear-drums rupture at an overpressure of $1.03 \times 10^5$ Pa.

The two people who suffered a ruptured ear-drum were located at a stand-off distance of 36.5 m from the explosion centre. If it is assumed that this stand-off distance corresponds to 50% of exposed ear-drums rupture, then the incident overpressure Ps was $1.03 \times 10^5$ Pa.

For a free field spherical TNT charge, an overpressure of $1.03 \times 10^5$ at 36.5 m is obtained for a mass of 1500 kg.

### 9.4. Motion of the witness riding a bike

The witness was riding at 60 m from the epicentre, he was projected 13 to 18 m away. It has been possible to calculate several possible trajectories and the corresponding pressure impulses. The fact that the witness was not injured gives limits that were not exceeded during the event (maximum over pressure, acceleration and impact velocity), helping to select a reduced set of more probable overpressure curves which were compared to the one obtained from other simulations.

### 9.5. Flying of steel piece No. 47 (beam from the cold box)

Flying of a beam from the cold box structure 12 m long, weighing 370 kg and found 575 m away, could not be used in spite of the good knowledge of the initial

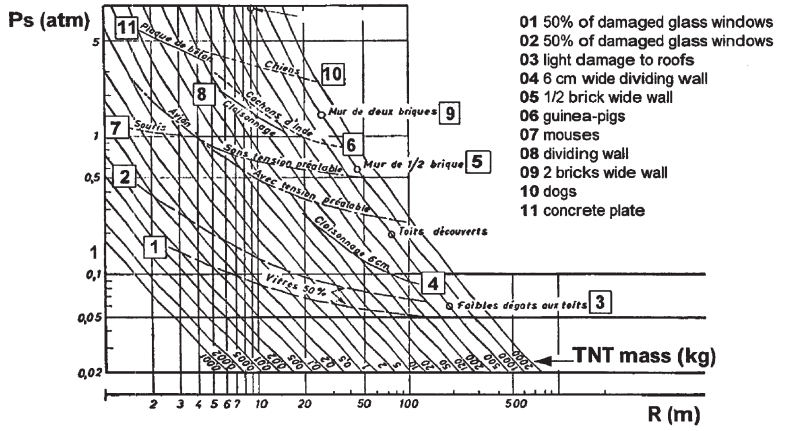


Fig. 11. TNT explosion: incident overpressure versus distance.

and final positions. This was due to the large uncertainties regarding both its flying position and its connection to the casing plates at the initial moment. For instance if the beam has flown like a javelin, its initial velocity could be 77 m/s, when this velocity would be supersonic if it has flown transversally.

### 9.6. Tilting of the CT 607 tower

The energy given to the column was able to rupture six of the eight anchor bolts. This energy is simple to evaluate knowing the dimensions and material of the bolts. The column was supported tilted at an angle of 20° by some light equipment close to its base. This led to the conclusion that the energy given to the explosion strength had not been much above the minimum required to break the bolts. This gives a value of the pressure impulse, pressure × time (triangular signal), of the blast at the location of this equipment.

### 9.7. Structural damage to the high pressure column

The blast was able to buckle the support skirt, as well as the centre of the upper head, but only very slightly buckle the column shell (Fig. 12). This can be used to evaluate the maximum pressure of the blast.

Finite element modelling of these structures has been performed using a static elastic model, a static elastoplastic model, and a dynamic elastoplastic model (LS-DYNA software). Calculations with these various models gave very different results and showed that the elastic model (not taking into account the yield stress) was far too coarse and gave unrealistic resistance to buckling and that only the elastoplastic model was realistic. Furthermore, dynamic modelling had to be considered to study the response of these structures to fast pressure variations on the column top.

A surprising observation is that the MP column has remained vertical and that the skirt collapsed about uniformly even though the weak points of the structure, the manholes of the skirt, were located on one side of the column. This was represented by prescribing a vertical displacement to the column instead of a free movement (Fig. 13).

Fig. 12. HP column, buckled skirt.

### 9.8. Fitting the reactive flow model

A reactive model has been used in order to calculate the pressure signal at the various distances of the selected markers: 0 m (HP column), 20 m (tilted water wash column), and 60 m (witness on a bicycle). The main parameters (unknowns of the problem) are the chemical energy, E, and the reaction time $\tau$ . The results of this

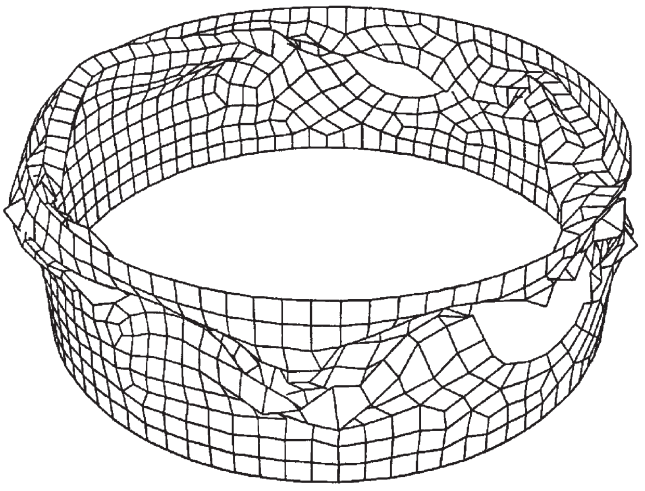

Fig. 13. HP column skirt, buckling pattern. Buckling of the higher head is shown in Fig. 14.

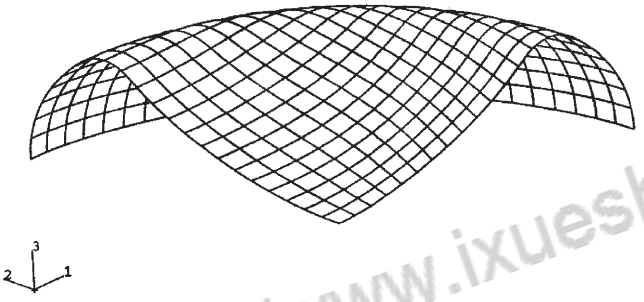


Fig. 14. HP column head, buckling pattern.

model, mainly the pressure and the velocity of gas as functions of time, are used as input for computing the mechanical effects on the receptor. The aim is to fit all observations with the same set of values E and $\tau$.

Table 2 gives the chemical energy, as a function of reaction time, which is necessary for having a blast consistent with the observed effects. Only a reaction time of 90 ms and a chemical energy of $8 \times 10^6$ kJ can explain simultaneously the three observations.

### 9.9. Aluminium mass involved in the reaction

The energy developed by the explosion, $8 \times 10^6$ kJ, is far too large to be explained by a hydrocarbon combustion, but it is consistent with an aluminium mass loss of 1700 kg and 5000 kg LOX in the vaporiser sump.

### 9.10. Partial conclusion

The aim of this part of the study was to estimate the level of energy released by the explosion (this explosion was a 'nonideal' detonation) and subsequently the TNT equivalence.

The deterministic method used to estimate the energy released by the explosion is based on numerical analysis and iterative computations between mechanical and reactive flow model. Computations give an energy of explosion equal to $8 \times 10^6$ kJ released in 90 ms. 1700 kg of burnt aluminium can explain the damage observed. In addition, if this energy is compared to that of TNT (4520 kJ/kg), the TNT equivalence in term of energy is equal to 1750 kg.

The TNT equivalence was also estimated according to a statistical approach based on window glass breakage and ear-drum rupture. This approach gives a TNT equivalence which ranges from 1000 to 2000 kg.

The main results are:

- Chemical energy = $8.10^6$ kJ;
- Reaction time = 90 ms;
- TNT equivalence = 1750 kg (in terms of chemical energy).

## 10. Ignition and propagation process

### 10.1. Ignition model

A simple model has been developed in order to investigate this process: the fins are coated with a hydrocarbon layer on each side, the oxygen layer is filled with boiling oxygen, the local liquid hold up can be expressed by means of a local liquid volume fraction (Fig. 15). A

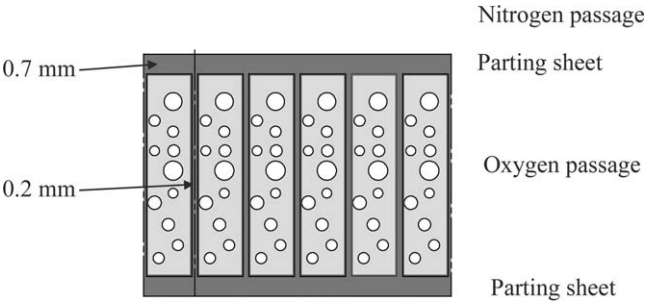


Fig. 15. Ignition model, fins coated with combustible.

Table 2
Chemical energy vs. reaction time

| Reaction time (ms) $\tau$ | HP column | Tilted water wash column | Witness on a bicycle |
|---|---|---|---|
| 9 | $E = 4 \times 10^6$ kJ | $E = 8 \times 10^6$ kJ | $E = 7 \times 10^6$ kJ |
| 90 | $E = 8 \times 10^6$ kJ | $E = 8 \times 10^6$ kJ | $E = 8 \times 10^6$ kJ |
| 900 | $E = 17 \times 10^6$ kJ | $E = 34 \times 10^6$ kJ | $E = 37 \times 10^6$ kJ |

Table 3
Ethylene promoted aluminium ignition, model. Theoretical temperature reached before aluminium combustion

| Liquid hold up ratio | Ethylene coating thickness (mm, both sides) | | | | | | | | | | | |
|---|---|---|---|---|---|---|---|---|---|---|---|---|
| | 0.02 | 0.04 | 0.06 | 0.08 | 0.1 | 0.15 | 0.2 | 0.25 | 0.3 | 0.35 | 0.4 | 0.45 |
| 0.005 | 803 | 1312 | 1144 | 1089 | 1085 | 1080 | 1076 | 1069 | 1067 | 1066 | 1065 | 1064 |
| 0.1 | 895 | 1833 | 1923 | 1901 | 1646 | 1285 | 1230 | 1206 | 1187 | 1173 | 1161 | 1150 |
| 0.2 | 692 | 1553 | 2089 | 2449 | 2750 | 2501 | 2072 | 1656 | 1454 | 1388 | 1344 | 1307 |
| 0.3 | 553 | 1286 | 1924 | 2231 | 2532 | 2815 | 2742 | 2492 | 2158 | 1805 | 1600 | 1510 |
| 0.4 | 451 | 1089 | 1716 | 2070 | 2330 | 2802 | 2897 | 2817 | 2657 | 2424 | 2108 | 1778 |
| 0.5 | 374 | 938 | 1496 | 1952 | 2179 | 2745 | 2868 | 2917 | 2848 | 2724 | 2541 | 2306 |
| 0.6 | 312 | 819 | 1322 | 1819 | 2063 | 2569 | 2825 | 2926 | 2923 | 2870 | 2753 | 2604 |
| 0.7 | 262 | 722 | 1179 | 1633 | 1972 | 2430 | 2784 | 2883 | 2945 | 2929 | 2873 | 2766 |
| 0.8 | 222 | 643 | 1062 | 1480 | 1895 | 2316 | 2739 | 2843 | 2934 | 2954 | 2936 | 2865 |
| 0.9 | 187 | 575 | 962 | 1348 | 1735 | 2222 | 2612 | 2807 | 2895 | 2954 | 2962 | 2927 |
| 1 | 159 | 518 | 877 | 1238 | 1597 | 2141 | 2503 | 2779 | 2860 | 2944 | 2979 | 2979 |

0.05 mm (25 g/m$^2$ × 2); ‘Classical’ explosions; Aluminium ignition (LOX excess); Aluminium ignition (aluminium excess).

shock ignites the hydrocarbon which burns with LOX. Table 3 shows the temperature reached by the three components at the end of the hydrocarbon combustion assuming that the fin has not reacted but has only interfered as a heat sink due to its enthalpy only (Fig. 16). Of course this model is a little rough, but it is based on a very fine mesh, as the fins are very close to each other (1.6 mm for 14 fins per inch). If this final temperature is far from the vaporisation temperature of aluminium, the fins will not be ignited, on the contrary, if it reaches 2000°C the fins will probably be ignited. This temperature depends on the quantity of local pollution and on the liquid present at the same place. A large amount of liquid will quench the reaction, a small amount of liquid will feed the reaction without quenching it.

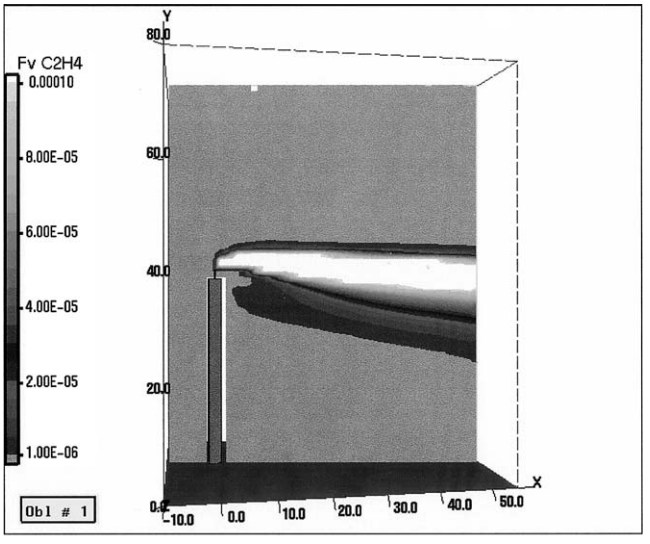


Fig. 16. Ethylene dispersion modelling, vent side.

This shock ignition model can explain how aluminium can be ignited independently and simultaneously in different layers.

### 10.2. Laboratory tests

Tests were conducted to check this theory. They were conducted on 0.2 mm corrugated aluminium discs of 19 mm diameter immersed in LOX. Ignition was triggered by 100 J shocks. [2] Of course most combustible materials are ignited in these conditions, but clean 0.2 mm thick aluminium sheets are not.

However, when the aluminium sheets had been polluted with a sufficient hydrocarbon coating, this low energy shock (100 J) could trigger aluminium ignition (Barthélémy et al., 2000).

The amount of LOX was controlled by means of the corrugation depth. Aluminium combustion was obtained when the hydrocarbon coating was 25 g/m$^2$ or more on each side of the discs. These conditions lead to about 1500°C in Table 3. This is consistent with the above theory considering the inaccuracy of both the theory and the experiments.

### 10.3. Hydrocarbon deposit assessment

In order to estimate the ethylene quantity required to ignite all LOX passages, the following approach was used:

- Perimeter of a channel 18 mm;
- Number of channels per passage: 504;
- Number of passages: 57 × 2.

[2] ASTM Standard D 2512-95.

If we suppose that 10% of the channels have been coated with an ethylene deposit of 0.025 mm on both sides on 100 mm height (see Fig. 7), this leads to a deposit of 18 × 504 × 57 × 2×0.1 × 100 = 258 552 $mm^3$. This volume corresponds to a mass of 250 g deposit.

Consequently, if ethylene is deposited along an edge of the cores, 250 g can be enough to instantly ignite aluminium in all passages.

Can this accumulation be achieved in 6 h with the exceptional pollution? This is the next question to be treated.

## 11. Hydrocarbon accumulation in the reboiler

### *11.1. Ethylene dispersion simulation*

Various simulations were made in order to assess the possible ethylene ingress into the cold box. The simulations made using the estimating software PHAST gave significant amounts. The first attempts made with a more precise simulation tool could hardly explain 1 ppmv ethylene pollution at air intake as the polluted plume was flowing horizontally and flying over the air intake which was located 10 m below. This could not explain the accident at all. The results became totally different when the columns located below the venting point were described in the model: the ethylene plume was then 'sucked down' and reached the air intake, giving concentrations ranging between 10 and 40 ppmv of ethylene. (Figs. 17–19). Of course the wind did not remain constant during the whole venting and, the plume did not hit the air intake during a part of this time. Consequently, 20 ppmv seems to be a reasonable value.

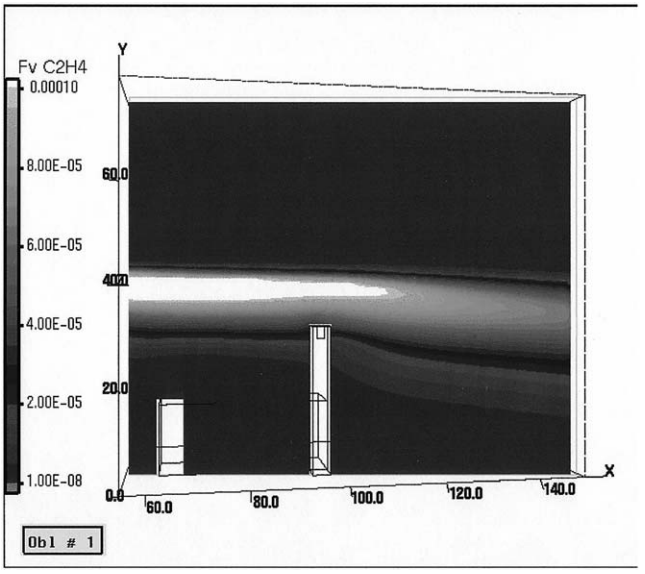


Fig. 17. Ethylene dispersion modelling, air intake side.

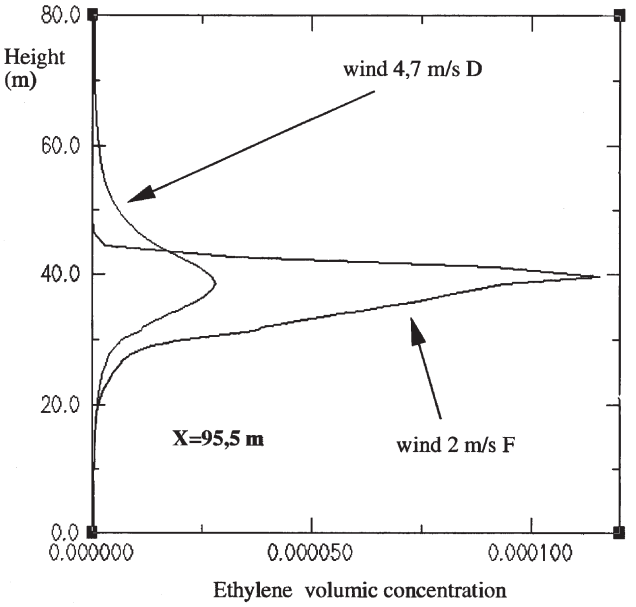


Fig. 18. Ethylene dispersion modelling, concentration profiles at the air intake.

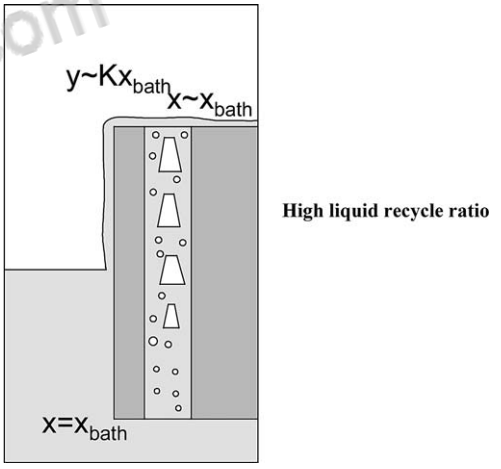


Fig. 19. Thermosiphon reboiler, normal operation.

As ethylene is partly adsorbed by the molecular sieve the average ethylene concentration entering the cold can have reached a value of 5 ppmv. Taking the simulations into account, this figure is of course associated to a large uncertainty.

### *11.2. Dry boiling*

A low level in the bath may cause dry boiling in the reboiler cores. This is a possible impurity accumulation process. This mechanism is illustrated by the following figures. The following variable names are used: x, impurity concentration in the liquid; y, impurity concentration in the vapour; K, equilibrium coefficient y/x (for ethylene 0.002); s, solubility limit of the impurity (for ethylene in LOX 13 000 ppm = 0.013 mole/mole).

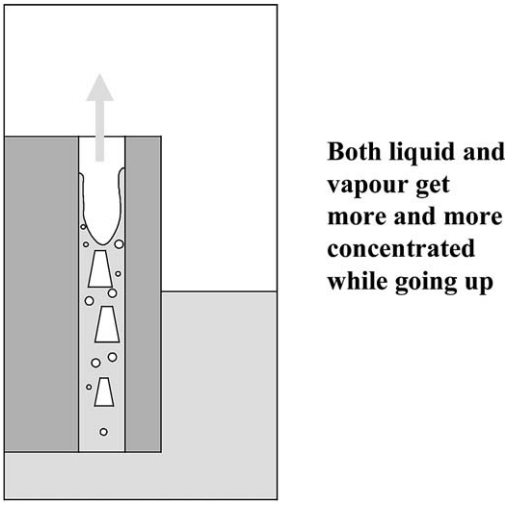


Fig. 20. Dry boiling.

In normal operation (Fig. 19) the liquid recycle ratio is high, the liquid concentration is about constant in the liquid loop, the vapour concentration is in equilibrium with the bath, y = K.xbath.

If the bath level is very low the lifting effect of the gas bubbles becomes insufficient to bring the liquid up to the passage top, and a dry boiling zone will appear (Fig. 20).Both the liquid and vapour get more concentrated while going up instead of remaining constant. Fig. 21 shows the equilibrium at the dry boiling zone interface when solid deposition occurs: the vapour concentration is limited by the equilibrium to a maximum concentration y = K.s. Fig. 22 illustrates the limit case where the liquid concentration is just below the solubility limit with no solid deposition : in this case the vapour concentration is both equal to the bath concentration to respect the material balance through the channel ($y = x_{bath}$) and to the previous value (y = K.s) to respect the liquid vapour equilibrium.

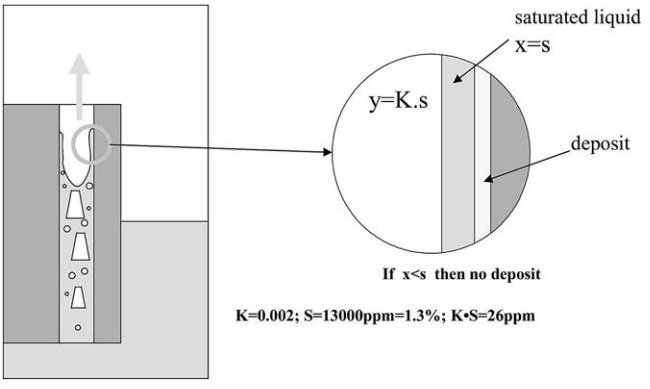


Fig. 21. Dry boiling with solid deposit.

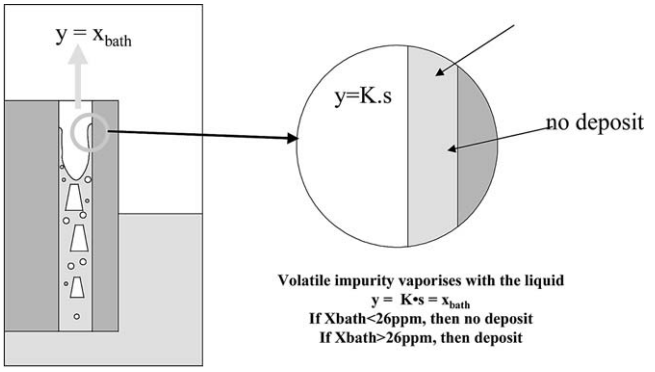


Fig. 22. Dry boiling with maximum concentration without deposit.

### *11.3. Impurity concentration of the outgoing gaseous oxygen outlet*

Using the previous relationships it is possible to illustrate the pollutant concentrations in the outgoing oxygen in typical cases (Fig. 23).

### *11.4. Possible concentration process*

The value of the ethylene concentration in the air entering the cold box downstream the front end purification makes it possible to calculate ethylene concentration maps in the vaporiser and the corresponding deposits according to various assumptions:

1. Dry boiling in all LOX channels with normal operation of the LOX adsorber (10% of the air flow rate);
2. Dry boiling in all LOX channels with no operation of the LOX adsorber (0% of the air flow rate);
3. Dry boiling in 10% of LOX channels with normal operation of the LOX adsorber (10% of the air flow rate);
4. Dry boiling in 10% of LOX channels with degraded operation of the LOX adsorber (2% of the air flow rate);
5. Dry boiling in 10% of LOX channels with no operation of the LOX adsorber (0% of the air flow rate) (see Fig. 24).

Cases 1 and 2 show that, whatever the operation of the LOX adsorber, no deposit at all occurs if dry boiling takes place in all channels, this is due to solubility and volatility properties of ethylene in LOX. Cases 3, 4 and 5 show that, when dry boiling is taking place in 10% of the channels only, deposition always occurs, whatever the operation of the LOX adsorber. Case 3 can be considered the most likely for the following reasons:

- There was no indication at all that the adsorber was not in line and analyses have shown presence of ethylene on the adsorbent;
- The low level has probably caused dry boiling in the

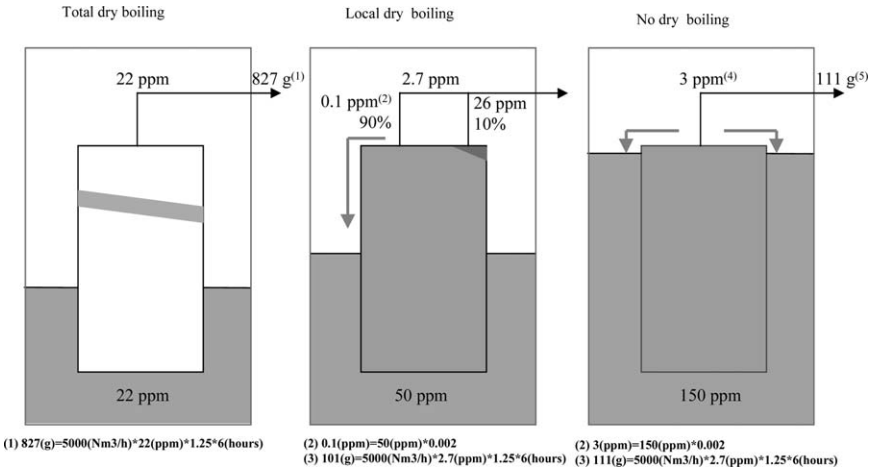


Fig. 23. Ethylene deconcentration by gaseous oxygen production.

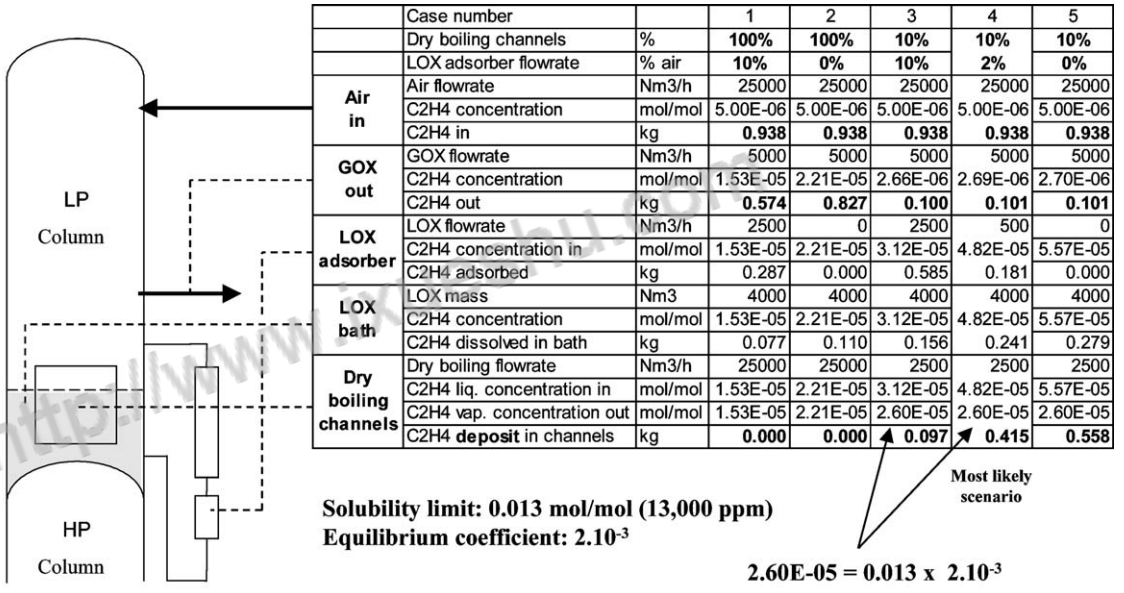


| | Case number | | 1 | 2 | 3 | 4 | 5 |
|---|---|---|---|---|---|---|---|
| | Dry boiling channels | % | **100%** | **100%** | **10%** | **10%** | **10%** |
| | LOX adsorber flowrate | % air | **10%** | **0%** | **10%** | **2%** | **0%** |
| **Air in** | Air flowrate | Nm3/h | 25000 | 25000 | 25000 | 25000 | 25000 |
| | C2H4 concentration | mol/mol | 5.00E-06 | 5.00E-06 | 5.00E-06 | 5.00E-06 | 5.00E-06 |
| | C2H4 in | kg | **0.938** | **0.938** | **0.938** | **0.938** | **0.938** |
| **GOX out** | GOX flowrate | Nm3/h | 5000 | 5000 | 5000 | 5000 | 5000 |
| | C2H4 concentration | mol/mol | 1.53E-05 | 2.21E-05 | 2.66E-06 | 2.69E-06 | 2.70E-06 |
| | C2H4 out | kg | **0.574** | **0.827** | **0.100** | **0.101** | **0.101** |
| **LOX adsorber** | LOX flowrate | Nm3/h | 2500 | 0 | 2500 | 500 | 0 |
| | C2H4 concentration in | mol/mol | 1.53E-05 | 2.21E-05 | 3.12E-05 | 4.82E-05 | 5.57E-05 |
| | C2H4 adsorbed | kg | 0.287 | 0.000 | 0.585 | 0.181 | 0.000 |
| **LOX bath** | LOX mass | Nm3 | 4000 | 4000 | 4000 | 4000 | 4000 |
| | C2H4 concentration | mol/mol | 1.53E-05 | 2.21E-05 | 3.12E-05 | 4.82E-05 | 5.57E-05 |
| | C2H4 dissolved in bath | kg | 0.077 | 0.110 | 0.156 | 0.241 | 0.279 |
| **Dry boiling channels** | Dry boiling flowrate | Nm3/h | 25000 | 25000 | 2500 | 2500 | 2500 |
| | C2H4 liq. concentration in | mol/mol | 1.53E-05 | 2.21E-05 | 3.12E-05 | 4.82E-05 | 5.57E-05 |
| | C2H4 vap. concentration out | mol/mol | 1.53E-05 | 2.21E-05 | 2.60E-05 | 2.60E-05 | 2.60E-05 |
| | C2H4 **deposit** in channels | kg | **0.000** | **0.000** | **0.097** | **0.415** | **0.558** |

**Most likely scenario**

**Solubility limit: 0.013 mol/mol (13,000 ppm)**
**Equilibrium coefficient: $2.10^{-3}$**

**$2.60E\text{-}05 = 0.013 \times 2.10^{-3}$**

Fig. 24. Bath concentration, accumulation in 6 h.

auxiliary reboiler and consequently reduced the LOX flow rate through the adsorber to about 2% of the air flow rate.

The resulting amount of deposit is about 400 g, which is consistent with the estimation made from observation of the reboiler remains. It was these observations that suggested dry boiling or reflux occurring only in a part of the channels.

Dry boiling in a part of the channels can have been caused by the level position: dry boiling in 100% of the LOX channels means a very low submergence, dry boiling in 0% of the LOX channels means a sufficient submergence to ensure a sufficient boiling in all channels. Local dry boiling at the top of certain channels only can be obtained at a very specific core submergence, probably not far from 50%, when most of the channels are still operating satisfactorily and when the least heated ones (due to slightly uneven heating) start having no positive liquid flow at their outlet.

### *11.5. Partial conclusion*

The ethylene venting can have been a sufficient pollution source to explain the explosion if the level was at a specific position allowing dry boiling in a limited number of the channels of most of the core passages.

## 12. General conclusion

### *12.1. Causes of the accident*

It can be concluded that the accident resulted from an exceptional pollution peak due to venting of ethylene

during a shut down of the ethylene plant, together with a low level in the ASU LOX reboiler bath, at reduced capacity. This was helped by the following unfavourable conditions:

1. The ASU was unusually kept in operation at reduced capacity during the ethylene oxide plant shut down.
2. Wind was blowing in an unusual direction, i.e. exactly from the ethylene vent to the air intake located 100 m downstream, but 10 m lower.

### *12.2. Magnitude of the explosion*

The hydrocarbon pollutant acted as an igniter, the actual fuel was aluminium, i.e. the reboiler material. A few hundreds of grams of ethylene were able to ignite more than 1000 kg of aluminium in LOX, multiplying the explosion energy by more than 1000.

### *12.3. Mechanisms*

In a BAHX LOX reboiler the most vulnerable parts to aluminium ignition are the fins. Fire can propagate within a single passage burning the fins only and without piercing the parting sheets to start with. This explains why a local pollution of a single passage can lead to limited explosions only. On the contrary, when a number of passages are polluted, the shock wave resulting from an explosion in a passage can instantaneously and simultaneously ignite aluminium in all other polluted passages leading to a massive runaway as verified experimentally (Barthélémy et al., 2000). The critical deposit allowing aluminium ignition in LOX is in the range of 25 g/m$^2$ of hydrocarbons on the fins.

A striking fact is the rapidity of the rise of the pollutant concentration in the reboiler cores. Although it is impossible to exclude other pollution sources or previous accumulation, it is reasonable to admit that a critical ethylene deposit, capable of igniting aluminium simultaneously in all LOX passages (i.e. 300 to 500 g), was accumulated in only 6 h. This is very surprising: even with the very high pollution experienced in this accident, ethylene is both soluble enough in LOX and volatile enough not to deposit at all in the reboiler cores, not only with a normal level but also with a low level causing dry boiling in all vaporisation channels. Dry boiling must then have taken place in a limited number of channels only, in each one of the polluted passages.

It appears that, for a given capacity, there is a precise level where fast deposition of impurities can take place in specific locations at the top of the reboiler cores, making it possible to accumulate critical deposits with a very limited amount of pollutant and consequently within a very short time, in situations where generalised dry vaporisation only would take a very long time to reach a critical accumulation or would not lead to any deposits at all.



## References

van Hardeveld, R. M., Bull, D., Groeneveld, M. J., & Lehman, J. Y. (2001). *Journal of Loss Prevention, 14*, 167–180.

Hirsh, S. F. (1968). The effects of overpressure on the ear drum, a review. *Annals of the New York Academy of Sciences, 152*, 147.

Barthélémy, H., Roy, D., Mazloumian, N. Ignition of aluminum by impact in LOX. Influence of contaminants, flammability and sensitivity of materials in oxygen enriched atmospheres, ninth nolume, ASTM STP 1395, August, 2000.

---

**阅读此文的还阅读了：**

1. Explosion indicator for explosion-proof enclosures
2. 商河县农村现代化研究(1997-2006)
3. 卷尺(1997型)
4. 《大英百科年鉴1997·表演艺术·音乐》翻译实践报告
5. Investigation of the Fushun ASU explosion in 1997
6. Investigation of the Fushun ASU explosion in 1997
7. 论邓小平的社会理想观（1975-1997）
8. 布莱尔政府时期的英国安全战略(1997-2007年)
9. Experimental investigation of external explosion in the venting process
10. 笔(1997型)
11. 《中国体育报》和《体坛周报》比较研究(1988-1997)
12. 瓶贴(金装1997)
13. Experimental and Numerical Investigation into the Internal Blast in Explosion Chamber
14. 香港电影（1997-2006）美学精神初探
15. Explosion indicator for explosion-proof enclosures
16. An Explosion in CNPC Fushun Petrochemical
17. Experimental investigation of p-section concrete beams under contact explosion and close-in explosion conditions
18. 中澳人权对话1997—2007
19. E-music Explosion
20. 1997-2007年美国对香港政策研究
21. EXPLOSION TREATMENT SYSTEM AND EXPLOSION TREATMENT METHOD
22. Investigation of Combustion and Explosion in Gaseous Suspensions Of Reactive Materials
23. Dust Explosion Hazards
24. 回归后香港电影表演文化研究（1997-2012）
25. 新工党治下英国的地区化进程(1997-2010年)

26. Steam Explosion in Microalgae Biorefining

27. 卷尺(1997-1型)

28. 笔盒(1997型)

29. Impact of China-Nigeria Relations in Nigeria from1997-2009

30. Investigation of the Fushun ASU explosion in 1997 [Journal of Loss Prevention in the Process Industries 16 (2003) 209-221]

31. 《人民日报》（1997-2016）对香港形象的建构研究

32. Quantitative Method of the Structural Damage Identification of Gas Explosion Based on Case Study:The Shanxi “11. 23” Explosion Inv

33. 重庆现代建筑研究（1978-1997）

34. EXPLOSION PROOF ENCLOSURES

35. E-music Explosion

36. Numerical and Experimental Investigation into Plane Charge Explosion Technique

37. 英国的公共外交(1997-2009)

38. Quantitative Method of the Structural Damage Identification of Gas Explosion Based on Case Study：The Shanxi “11. 23” Explosion In

39. Explosion in Disputes

40. 内蒙古汉语儿童小说主题分析（1947-1997）

41. 论英国对香港政策及其影响（1997-2016）

42. 论东盟对中美的对冲战略(1997~2008)

43. 《大英百科年鉴1997·文学》翻译实践报告

44. Numerical and Experimental Investigation into Plane Charge Explosion Technique

45. EXPLOSION PROTECTION DEVICE FOR EXPLOSION-DECOUPLING OF TWO PARTS OF A PLANT

46. 伊朗对美外交政策探析(1997—2007)

47. Investigation of the Fushun ASU explosion in 1997 [Journal of Loss Prevention in the Process Industries 16 (2003) 209-221]

48. 邓小平军队政治工作思想研究（1975-1997）

49. Experimental investigation of external explosion in the venting process

50. 西部地区某县取保候审实证研究:1997-2012